

# STUDY ON REDUCING AND MELTING BEHAVIOR OF MILL SCALE/PETROLEUM COKE BLEND

Bruno Deves Flores <sup>1</sup>  
Ismael Vemdrame Flores <sup>1</sup>  
Maurício Covcevich Bagatini <sup>2</sup>  
Eduardo Osório <sup>3</sup>  
Antônio Cezar Faria Vilela <sup>4</sup>

## Abstract

Self-reducing tests were carried out under isothermal and non-isothermal condition in a muffle furnace, aiming to assess the reduction and melting of a self-reducing blend of mill scale and petroleum coke (85-15% in weight). The products obtained were analyzed by mass loss and wet analysis. Further investigations for the products from the non-isothermal condition were done by X-ray diffraction, nude eye inspection and carbon analyzer. It was observed that mass loss fraction and metallization degree are directly related and both increase with time and temperature. In the non-isothermal maximum mass loss was achieved in 8 minutes, reaching metallization degrees above 90%. It was observed that the reduction of iron oxide occurs mainly in solid state and the smelting of the samples is directly related to the iron carburization process. Thus, the use of self-reducing mixtures shows a possible way to recycle mill scale.

**Keywords:** Mill scale; Self-reduction; Iron carburization.

# ESTUDO DO COMPORTAMENTO DE REDUÇÃO E FUSÃO DE MISTURAS DE CAREPA/COQUE DE PETRÓLEO

## Resumo

Testes de autorredução em condições isotérmicas e não isotérmicas em forno mufla, foram propostos para avaliar a redução e fusão de uma mistura autorredutora de carepa e coque de petróleo (85-15% em massa). Os produtos obtidos foram analisados através de análises de perda de massa e via úmida. Para os produtos obtidos nas condições não isotérmicas também foram realizadas análises de difração de raios-X, inspeção a olho nu e análise de carbono. Observou-se que a fração reagida e o grau de metalização obtidos estão diretamente relacionados e ambos aumentam com o tempo e temperatura. Os ensaios não isotérmicos levaram 8 minutos para atingir a perda de massa máxima da mistura, alcançando graus de metalização superiores a 90%. Verificou-se que a redução dos óxidos de ferro ocorre principalmente no estado sólido e que a fusão das amostras está diretamente relacionada com o processo de carburação do ferro. Desta forma, o uso de misturas autorredutoras indica uma possibilidade de reciclagem de carepa.

**Palavras-chave:** Carepa; Autorredução; Carburação do ferro.

<sup>1</sup>Metallurgical Engineer, Laboratório de Siderurgia – LASID, Universidade Federal do Rio Grande do Sul – UFRGS, Porto Alegre, RS, Brasil. E-mail: bruno.flores@ufrgs.br; ismael.flores@ufrgs.br

<sup>2</sup>Metallurgical Engineer, Dr., Professor, Department of Metallurgical Engineering, Universidade Federal de Minas Gerais – UFMG, Belo Horizonte, MG, Brasil. E-mail: bagatini@demet.ufmg.br

<sup>3</sup>Metallurgical Engineer, Dr., Professor, Laboratório de Siderurgia – LASID, Universidade Federal do Rio Grande do Sul – UFRGS, Porto Alegre, RS, Brasil. E-mail: eosorio@ct.ufrgs.br

<sup>4</sup>Metallurgical Engineer, Dr-Ing., Professor, Laboratório de Siderurgia – LASID, Universidade Federal do Rio Grande do Sul – UFRGS, Porto Alegre, RS, Brasil. E-mail: vilela@ufrgs.br

## 1 INTRODUCTION

The iron oxide scale, formed on the surface of steel, is one of the wastes generated in steel plants and represents about 2% of the produced steel [1]. It is formed during the continuous casting and rolling mill processes when steel is submitted to thermal gradients in oxidant atmospheres, which promotes the growth of iron oxides layer at the surface of steel. Such a scale is very rich in iron (~70%) and generally contains wüstite as predominant iron oxide phase, followed by magnetite and hematite [2,3].

In integrated steel plants, the mill scale is habitually used as raw material at sintering plants but the recycling of this waste has also been reported in the form of briquettes used in BOF steelmaking [1,4,5]. In the case of mini-mills plants which operate using electric arc furnaces (EAF) and where there are no reduction reactors, the scale recycling is more difficult and this waste is often sent to landfills or used by the cement industry. However, the possibility of using self-reducing composites as a part of the charge in traditional processes such as EAF has opened new ways to recycle ironmaking and steelmaking waste. Some authors have already reported this possibility, but the details are still being investigated [6-8].

The self-reduction basically consists of an intimate mixture of iron oxides and carbonaceous materials so that, when under heating at high temperatures, the carbon content in the agglomerate is sufficient to obtain metallic iron. The mechanism of the self-reduction process has been widely studied over the past few years, and it involves chemical reactions and phenomena of mass and heat transfer [6,9-12]. The main chemical reactions during the heating of self-reduction mixtures are the reduction of iron oxides via gas and gasification of the carbonaceous materials (Boudouard reaction). As these reactions occurs concurrently, one or the other can control the overall reaction rate in the self-reducing composites, depending on a variety of experimental conditions such as composition ( $\text{Fe}_x\text{O}_y/\text{C}$  ratio), shape (pellet, briquette, packed bed) and size of agglomerate, heating conditions and the composition and pressure of the surrounding atmosphere. The kinetic of both reactions has been studied as a tool to the determination of the controlling step of the global process of self-reduction [9-12].

On the other hand, the mechanism of melting of reduced iron is still underexplored and a better understanding in this field is an important issue lights of energy savings in metallurgical process [13]. The melting of iron is associated with a number of factors, including its carburization, since the melting temperature is a function of carbon content in the iron. Ohno *et al.* [14] proposed that the reduced iron carburization of self-reduction materials at high temperatures may occur primarily through three different ways: direct carburization, gas carburization and carburization during the smelting-reduction. In a similar study, Kim *et al.* [15] observed an increase in the

rate of iron melting during the formation of Fe-C phase in simultaneously contact with carbon and wüstite. The contribution of a gas phase in carburization has also been studied, and focused on kinetics of this process [16-18]. Iguchi and Endo [19] showed that the iron formed from self-reducing pellets is carburized mostly by direct carburization,  $C_{(s)} = [\text{C}]$ , which occurs through the contact of carbonaceous particles and reduced iron.

In light of this, the present work aimed to assess the reducibility and metallic yield of self-reducing mixture comprised of mill scale and petroleum coke, as well as to measure the carburization of the iron products formed. Therefore, this study is a part of long-term project to get an inside on the possibility to use self-reducing blends/agglomerates in electric arc furnace. The scale used in this work was first characterized and its reduction behaviour in pure CO and CO-CO<sub>2</sub> mixtures was investigated [3].

## 2 EXPERIMENTAL

### 2.1 Raw Materials and Self-Reducing Blends Preparation

The production of self-reducing blends was carried out with mill scale and petroleum coke. The scale used was provided by a Brazilian mini-mill plant and was sampled and composed according to the proportion generated in continuous casting (25% mass) and rolling mill (75% mass). Its chemical characterization (Table 1) was performed by Mössbauer spectroscopy (ferrous components) and inductively coupled plasma atomic emission spectroscopy (trace components). The determination of oil and moisture content was performed by mass loss before and after heating. More details of this characterization can be found in a previous work [3].

The petroleum coke chosen as reducing agent was characterized via proximate analysis (Table 2). The chemical characteristics (high fixed carbon and low ash content) of this material and its availability were the reasons for this choice.

Particle size analysis was carried out for both materials. Samples of 250 g were submitted to dry sieving in wire cloth sieves with square openings (2.37, 0.84, 0.42, 0.25, 0.15, 0.11, and 0.07 mm). The sieve analysis was performed using a mechanical sieve shaker and sieving time of 20 minutes was applied. The particle size range of each material is shown in Figures 1 and 2.

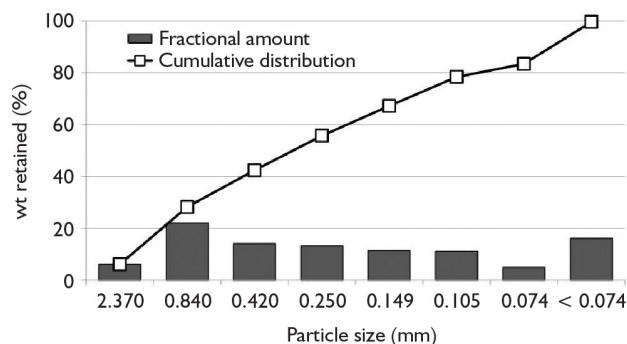
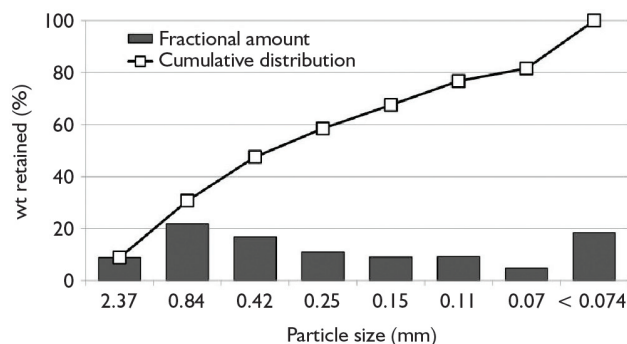
To prepare the self-reducing blends, the molar ratio of  $O_{\text{reducible}}/C_{\text{fixed}} = 1$  was established, i.e. all the carbon was considered to lead the formation of CO. Thus, the blends were comprised of 85% of mill scale and 15% of pet coke in weight. Mixtures of 50 g were packed in plastic bags (Figure 3), which were used only to facilitate the charging

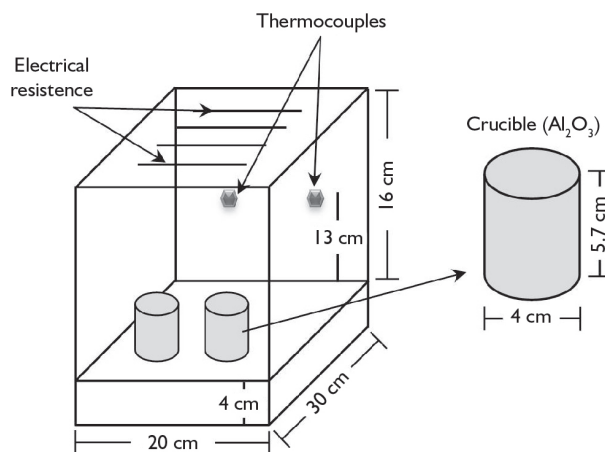
**Table 1.** Mill scale composition

Constituents	Fe <sub>2</sub> O <sub>3</sub>	Fe <sub>3</sub> O <sub>4</sub>	FeO	Fe <sup>0</sup>	Moisture	Oil	Contaminants/Others
wt %	3.8	33.8	53.4	0.3	6.0	0.3	2.4

**Table 2.** Petroleum coke composition

Constituents	Moisture	Ash	Volatile Matter	Fixed Carbon
wt %	0.7	0.1	10.9	88.3


**Figure 1.** Size distribution of mill scale particles.

**Figure 2.** Size distribution of pet coke particles.

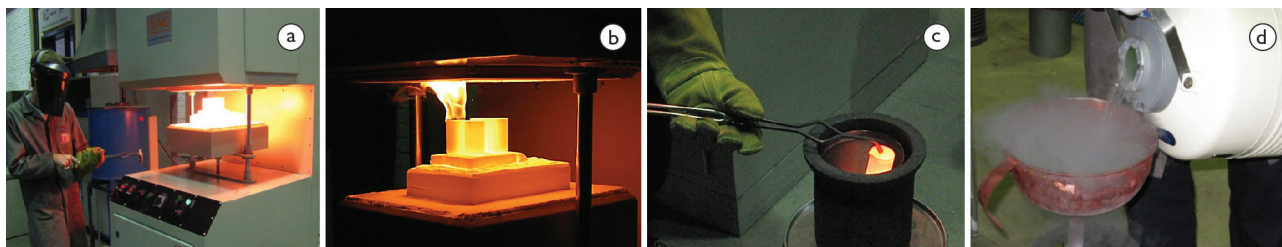
**Figure 3.** Self-reducing bag of mill scale and petroleum coke.

**Figure 4.** Schematic representation of muffle furnace and alumina crucible.

procedure during the self-reduction tests. It is important to notice that no compression of the blend was done to prepare the bags, once the objective was to eliminate the need of pre-agglomeration.

## 2.2 Self-Reduction Tests

The self-reducing tests were carried out in two different conditions, isothermal and non-isothermal. Both experiments were done using preheated alumina crucibles in a muffle furnace (Figure 4) under room atmospheric conditions. After reaching each preheating temperature the furnace (Figure 5a) was opened and the plastic bag was immediately loaded inside of the crucible without any cover (Figure 5b), then the furnace was closed and the heating was carried on. The plastic bag material was immediately burned out after charging. The complete procedure (open, charge and close the oven) took approximately 50 seconds. At the end of the residence time the samples were quenched in liquid nitrogen to stop self-reducing reactions and avoid the reoxidation of the formed products (Figure 5c and d).

The isothermal trials were carried out according to the heating profile shown in Figure 6. These experiments aimed to investigate the effect of temperature and time on the yield of self-reduction samples. Thus, the furnace was preheated up to 50°C above the test tempe-



**Figure 5.** Experimental procedure for the isothermal and non-isothermal self-reducing tests. (a) and (b) furnace opening and sample charging; (c) and (d) quenching procedure.

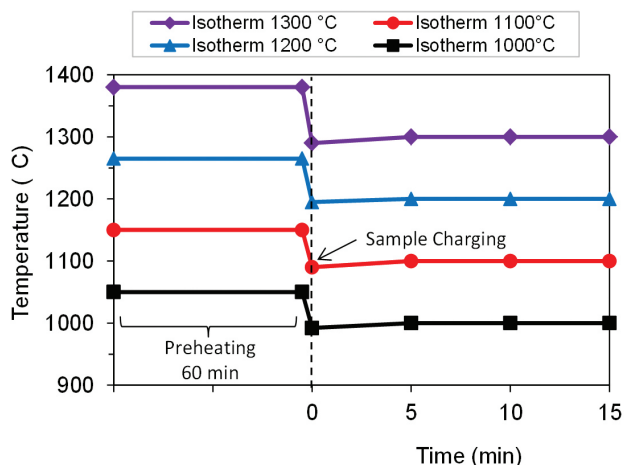


**Figure 6.** Heating profile of isothermal tests.

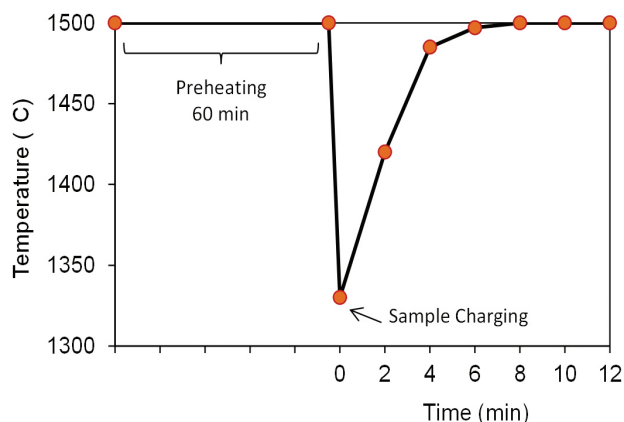


**Figure 7.** Heating profile of non-isothermal tests.

perature (1,000 °C, 1,100°C, 1,200°C and 1,300°C), once the procedure to open the furnace and charge the sample in the crucible dropped its temperature. The bags were introduced one at the time and the tests were interrupted for data collection at 5, 10 and 15 minutes. The products of these experiments were analyzed by mass loss and wet analysis.

The non-isothermal tests were performed aiming to investigate the self-reduction behavior of the blends at high temperatures. In these experiments the furnace was preheated up to 1,500°C (Figure 7) and then opened to charge the bags (one at a time), dropping the furnace temperature to approximately 1,320°C. Thus, the sample was subjected to a fast heating condition, from 1,320 to 1,500°C in 6 minutes and kept at 1,500°C for 6 more minutes. The tests were interrupted for data collection at 2, 4, 6, 8, 10 and 12 minutes.

The products obtained for each time were analyzed by mass loss, wet analysis, X-ray diffraction, naked eye inspection and carbon analyzer. The wet analyses was performed according to the methods described by Hughe *et al.* [20] Samples were scanned as powder on a glass slide using the Siemens/Bruker AXS D5000, with a copper anode x-ray tube from 2° to 72° using parallel beam optics, a 0.02° step size and 1 second count time. To measure only the carbon content in the reduced iron an ultrasonic cleaning with ethanol was necessary to separate fine residual carbonaceous particles attached in

the products. After cleaning the carbon content in the reduced iron was measured based on the combustion-infrared absorption method (ASTM E1019-11) [21], using a LECO CS-244. No statistical treatment was performed on all proposed analyses.

### 3 RESULTS AND DISCUSSION

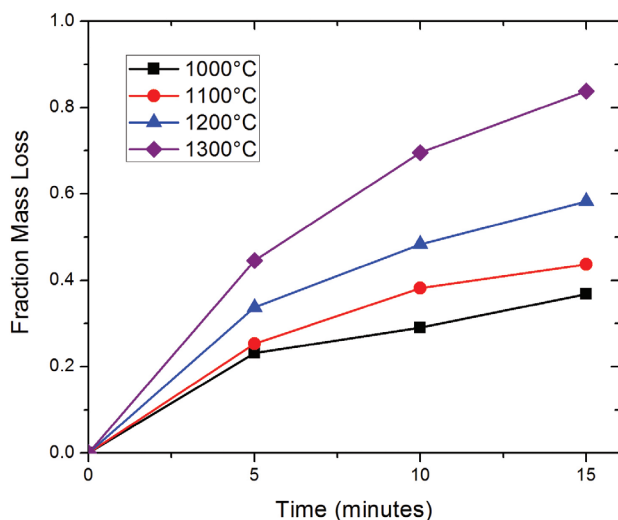
#### 3.1 Isothermal Tests

Figure 8 presents graphic of fraction mass loss versus time for the isothermal tests, where the fraction mass loss was calculated by the Equation 1:

$$\text{Fraction Mass Loss} = \frac{m_0 - m(t)}{m_0} \cdot \frac{1}{M_{\max}} \quad (1)$$

where  $m_0$  is the initial sample weight in grams,  $m(t)$  is the sample weight in grams at time  $t$  and  $M_{\max}$  is the maximum mass loss for the samples ( $M_{\max} = 0,39$ ), which was calculated by the maximum mass loss due the release of moisture, volatile matter, reducible oxygen and by the carbon gasification.

The results observed in Figure 8 indicate that as the temperature and time increase, the fraction mass loss increased for all samples tested. The mass loss occurs due the release of moisture of the blend, devolatilization of



**Figure 8.** Fraction mass loss for self-reducing blends under isothermal conditions.

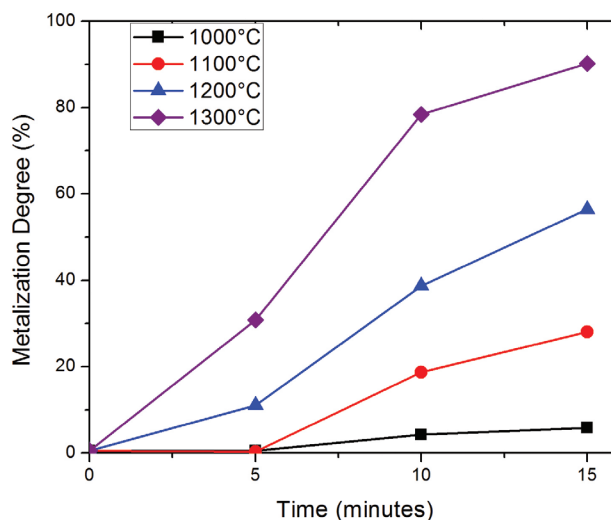


**Figure 9.** Metallization degree of the samples after isothermal tests.

petroleum coke and self-reduction reactions. In the first 5 minutes the rate of mass loss is higher compared with the subsequent times. This behavior may be result of the release of moisture and volatile matter that occurs faster than self-reduction reactions. The mass loss observed for 10 and 15 minutes occurs mostly by the self-reduction reactions (iron oxides reduction and carbon gasification). The higher values of fraction mass loss observed with increase of temperature are probably due to a higher formation of reducing gas and reduction of iron oxides.

Figure 9 shows the metallization degree ( $Fe^0/Fe_{total}$ ) versus time for the isothermal tests. The metallization degree was investigated to verify that mass loss also resulted in metallic iron gain. The metallization showed the same positive effect of time and temperature as observed for fraction mass loss. For all temperatures, the maximum metallization degree was reached at 15 minutes. At low temperatures, long periods of time are necessary to reach high metallization levels. On the other hand, at 1,300°C the samples show a relatively high metallization degree (30,8%) even for 5 minutes of test, probably because of the higher temperature that increases the rate of chemical reactions. [8]

The comparison between fraction mass loss and metallization degree for the first 5 minutes of the test suggests that for the lower temperatures (1,000°C and 1,100°C) the mass loss observed was mainly due the release of moisture and volatile matter, since it did not result in a metallic iron gain. For the higher temperatures (1,200°C and 1,300 °C) the same behavior was observed, nevertheless, due the better kinetic conditions the heating process also resulted in a metallic iron gain. This suggests that after the release of volatile matter the increase of fraction mass loss was directly related to the self-reduction reactions.

## 3.2 Non-Isothermal Tests

### 3.2.1 Fraction mass loss and metallization degree

The relationship of fraction mass loss to time and temperature in the non-isothermal tests is shown in Figure 10. The mass loss for the non-isothermal condition occurs for the same reasons as explained in section 3.1 (release of moisture, volatile matter and self-reducing reactions). However, due to the higher temperature of the test, the mass loss rate is higher and an approximately linear relationship was observed between time and fraction mass loss until 6 minutes. Such behavior may have resulted from the continuous increasing of temperature and time. The maximum fraction mass loss was achieved at 8 minutes, and after that the sample mass remained stable.

Figure 11 shows the metallization degree for non-isothermal tests. The rate of metallization begins slowly and increases significantly after 2 minutes. The initial mass loss does not reflect directly on metallization degree due to the release of volatile matter and moisture, as discussed in 3.1. In regards to the fraction mass loss, after 8 minutes the metallization degree also becomes relatively stable reaching values above 90%.

### 3.2.2 X-ray diffraction

The X-ray diffraction analysis was used to identify the phases present in the material during the reduction and melting processes. From the previous chemical characterization of the samples, it was known that iron oxides were the predominant substances in the mixture before tests and the amount of metallic iron is not significant. At 2 and 4 minutes (Figures 12a and b) the presence

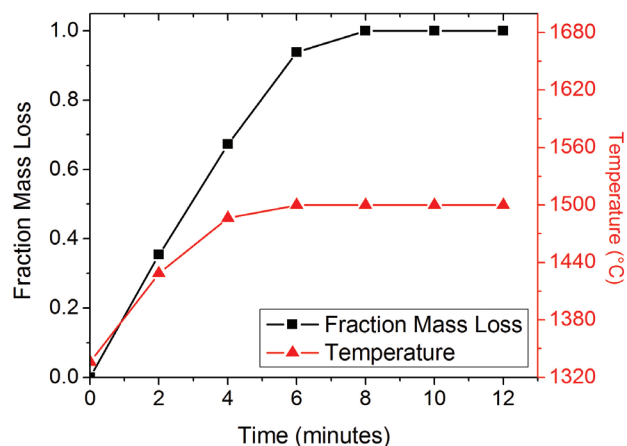


**Figure 10.** Fraction mass loss for self-reducing blends under non-isothermal conditions.

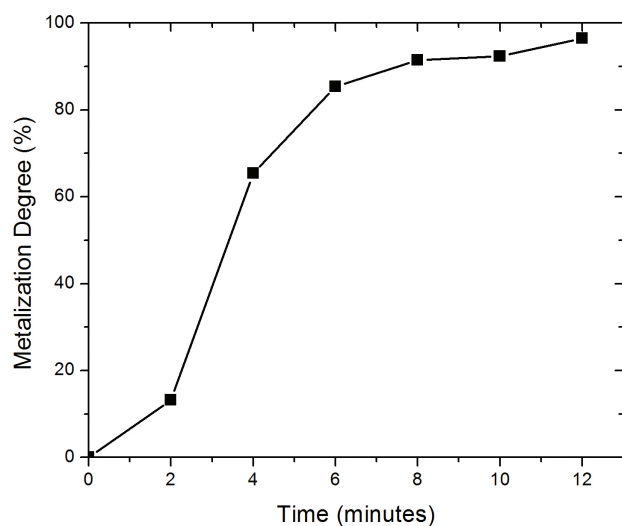


**Figure 11.** Metallization degree of the samples during non-isothermal tests.

of magnetite, wüstite and the appearance of metallic iron was recorded. For 6 minutes only wüstite and metallic iron were detected, indicating the complete reduction of magnetite. After 8 minutes only the presence of metallic iron was observed.

The metallization degree, which is shown in item 3.2.1, revealed that even after 8 minutes, there is no total metallic iron formation, which is in contrast to that shown in Figures 12d-f. This difference can be explained by the sensitivity of XRD analysis (5%), which might not have been able to detect the presence of little amounts of iron oxides.

### 3.2.3 Morphology and carbon content

The morphology of the formed products after the non-isothermal experiments was visually analyzed by the naked eye (Figures 13a-f). It was observed that until 4 minutes (Figures 13a and b) the products were formed

in solid state. After 6 minutes (Figure 13c), significant change occurred in the structure of the samples due the incipient melting of the reduced iron, in which the particles agglomerate and form a highly metalized, porous material. The main change observed between 8 (Figure 13d) and 10 minutes (Figure 13e) was the contraction of the samples due to the progressive increase of the liquid phase fractions. The complete melting of the samples (Figure 13f) was reached at 12 minutes.

The carbon contained in the reduced iron was investigated for 8, 10 and 12 minutes and are shown in Figure 14. The samples of 8 and 10 minutes show slight differences in the average carbon contained (0,29-0,22%, respectively). However, at 12 minutes this average is increases to 1,86%. Such behavior may be explained by the deficiency of carbon/iron contact for 8 to 10 minutes due to the dispersion of carbonaceous particles on the bottom of the crucible. However, as the liquid phase increase carbon and iron particles are able to interact again, increasing the amount of carbon contained in reduced iron, promoting a complete melting of the samples.

### 3.2.4 Reduction and melting behavior

Based on the previous results this item is proposed to explain the reduction, carburization and melting of the reduced iron for the non-isothermal tests. Immediately after the samples have being charged in the hot crucibles the self-reducing samples start to be heated up and the iron oxide reduction take place from the outer part forward to the core of the samples, as shown in Figure 15. Taking into account the results of metallization degree, XRD analyses and looking at the products it is possible to affirm that the larger part of the iron oxides reduction occurs in solid or semi-solid states, which takes place mostly before 8 minutes, suggesting that the gas/solid reaction is the mean mechanism for the reduction of the samples under the experimental conditions. However, it is important to notice that due to the experimental conditions the temperature during the non-isothermal experiment (Figure 7) was measure near to the furnace wall and not on the sample. Thus the contribution of heat transfer inside of the sample could not be evaluated and the reduction of the iron oxides could have occurred in lower temperature than that showed in Figure 7. During this first stage carburization occurs basically via gas and direct contact of carbonaceous materials with iron (Figure 15a).

After this first stage there is no more reductant gas (or little amounts) in the system and it was observed that part of the unreacted carbonaceous material is trapped between the partially melted regions and the remainder is dispersed at the bottom of the crucible without direct contact with the iron formed (Figure 15b). These parti-

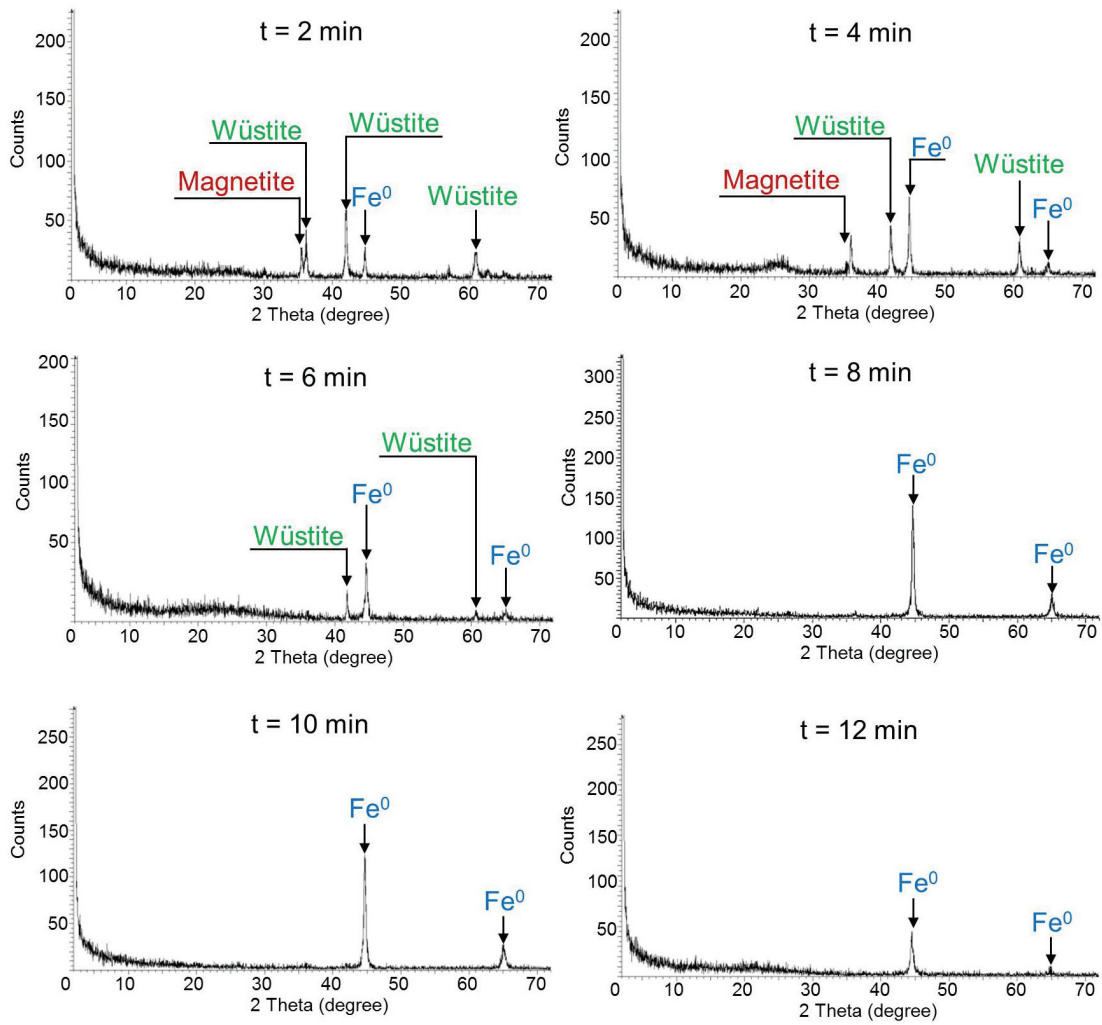


Figure 12. X-ray diffraction analyses for non-isothermal tests.

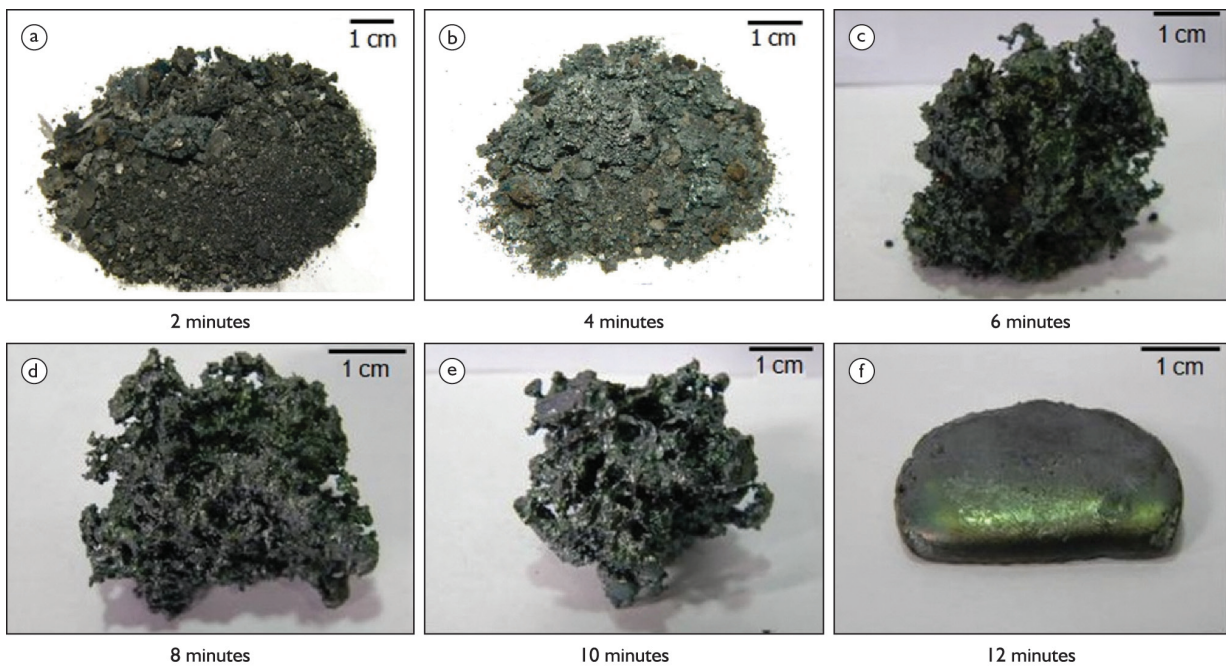


Figure 13. Sample appearance after non-isothermal tests.

cles are preferably comprised of coarse particles. The melting temperature of pure iron is 1,538°C at 1 atm, which is impossible to achieve under these experimental conditions. However, the increase of carbon contained in reduced iron decreases the alloy melting temperature. As was seen, during this period (from 8 to 10 minutes) the average carbon contained remained stable, under 0.3 wt %. It is believed that carbon distribution in the iron particles was not homogeneous (Figure 15b), once the periphery of the reduced iron particles seem melted while the core remained solid. As suggested by Murakami *et al.* [22], it is necessary an incubation time to melt iron by carburization, which is the time required for the carbon concentration to reach the supersaturated concentration and the driving force for this process is the

carbon diffusion. Once the carbon diffusion process allows an increase of iron liquid phase formation, because of the decrease of iron melting point, liquid phase formed interacted with the dispersed carbon particles at the bottom of the crucible, increasing the amount of carbon in the Fe-C alloy significantly, allowing the complete melting of the reduced iron (Figure 15c). Iguchi and Endo [19] concluded that coarse carbonaceous materials increase the final percentage of carbon contained in iron formed, once the fine particles of carbonaceous materials have a higher surface they are significantly more involved in the reduction step. On the other hand, coarse particles seem to remain in the system and effectively participate in the carburization of the reduced iron.

Therefore this study contributes with previous work [16] which assumed that the carburization of reduced iron particles occurs mainly by the direct carburization reaction,  $C(s) \rightarrow [C]$ , through direct contact points of carbonaceous particles and iron and controlled the melting process of the samples, under this experimental conditions.

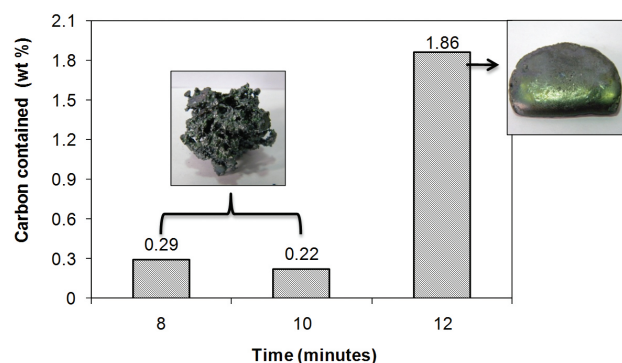


Figure 14. Carbon content of reduced iron.

#### 4 CONCLUSIONS

Based on the findings and considerations made throughout the study of the self-reducing blend of mill scale/pet coke, the following conclusions were obtained:

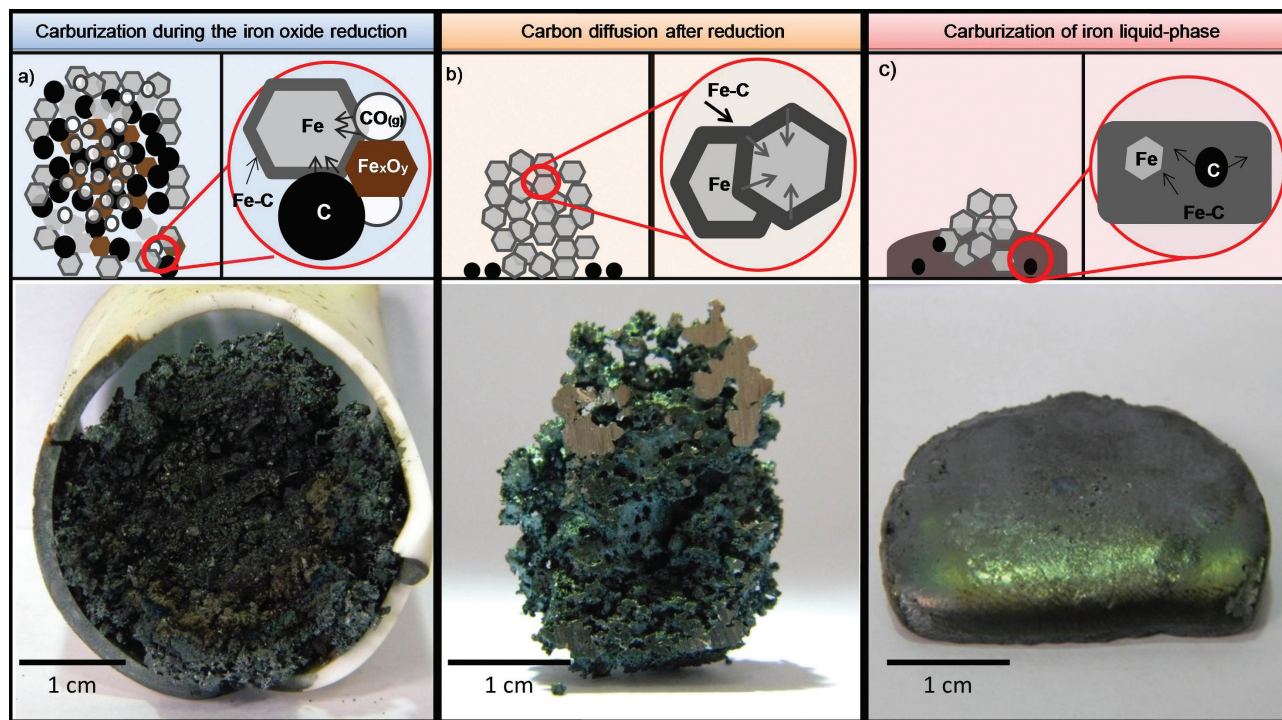


Figure 15. Schematic representation of reduced iron carburization and melting mechanism.

- The self-reduction of mill scale/pet coke samples showed a positive dependence on time and temperature. The fraction mass loss and the metallization degree were directly correlated;
- It was found that reduction of iron oxide at elevated temperatures (1,300°C-1,500°C) occurred mainly in solid state;
- The metallization degree levels (up to 90%) reached in non-isothermal conditions, showed a significant gain of metallic iron and a potential way to recycle scale;
- Three different morphologies were observed for the products formed on high temperature tests:

solid (2 and 4 minutes), partially melted (6, 8 and 10 minutes) and completely melted (12 minutes). It was found that the melting behavior of the self-reducing mixtures was directly related to the process of carburization of iron. The direct carburization ( $C_{(s)} = [C]$ ), was proposed as the main mechanism for the increase of carbon in iron.

### Acknowledgements

The authors acknowledge the financial support of CNPq and Capes.

### REFERENCES

- 1 Umadevi T, Sampath Kumar MG, Mahapatra PC, Mohan Babu T, Ranjan M. Recycling of steel plant mill scale via iron ore pelletisation process. *Ironmaking & Steelmaking*. 2009;36:409-415. <http://dx.doi.org/10.1179/174328108X393795>
- 2 Krzyzanowski M, Beynon JH, Farrugia DCJ. Oxide scale behavior in high temperature metal processing. Weinheim: Wiley - VCH; 2010. <http://dx.doi.org/10.1002/9783527630318>
- 3 Bagatini MC, Zyma V, Osorio E, Vilela ACF. Characterization and reduction behavior of mill scale. *ISIJ International*. 2011;51:1072-79. <http://dx.doi.org/10.2355/isijinternational.51.1072>
- 4 Balajee SR, Callaway PE Jr, Keilman LM. Production and BOF recycling of waste oxide briquettes containing steelmaking sludges. *Steelmaking Conference Proceedings*. 1995;78:51-65.
- 5 Nascimento RC, Lenz G, Martins D, Takano C, Mourão MB. Carbothermic reduction of self-reducing briquettes containing wastes from blast furnace and BOF sludges. In: ABM. Proceedings of the 5<sup>th</sup> Japan-Brazil Symposium on Dust Processing-Energy-Environment in Metallurgical Industries; 2004; Vitória, Brasil. São Paulo: ABM; 2004. p. 507-516.
- 6 Dukelow DA, Werner JP, Smith NH. Use of Waste Oxides in the Great Lakes BOP Steelmaking. In: Iron and Steel Society. Proceedings of the Steelmaking Conference; Nashville, EUA; 1995. Ann Arbor: ISS; 1995. p. 67-72.
- 7 Godinski NA, Kushnarev NN, Yakhshuk DS, Kotenev VI, Yu Barsukova E. Use of iron-carbon bearing briquettes in electric steelmaking. *Metallurgist*. 2003;47:16-19. <http://dx.doi.org/10.1023/A:1023818126564>
- 8 El-Hussiny NA, Shalabi MEH. A self-reduced intermediate product from iron and steel plants waste materials using a briquetting process. *Powder Technology*. 2001;205:217-23. <http://dx.doi.org/10.1016/j.powtec.2010.09.017>
- 9 Donskoi E, McElwain DLS, Wibberley LJ. Estimation and modeling of parameters for direct reduction in Iron ore/ coal composites: Part II - Kinetic parameters. *Metallurgical and Materials Transactions B*. 2003;34B:255-66.
- 10 Fortini OM, Fruehan RJ. Rate of reduction of ore-carbon composites: Part II - Modeling of reduction in extended composites. *Metallurgical and Materials Transactions B*. 2005;36B:709-17.
- 11 Coetsee T, Pistorius PC, Villiers EE. Rate-determining steps for reduction in magnetite-coal pellets. *Mining Engineering*. 2002;15:919-29. [http://dx.doi.org/10.1016/S0892-6875\(02\)00120-6](http://dx.doi.org/10.1016/S0892-6875(02)00120-6)
- 12 Sun K, Lu W-K. Mathematical modeling of the kinetics of carbothermic reduction of iron oxides in ore-coal composite pellet. *Metallurgical and Materials Transactions B*. 2009;40B:91-103.
- 13 Ohno K, Milki T, Hino M. Kinetic Analysis of iron carburization during smelting reduction. *ISIJ International*. 2004;44(12):2033-39. <http://dx.doi.org/10.2355/isijinternational.44.2033>
- 14 Ohno K, Milki T, Sasaki Y, Hino M. Carburization degree of iron nugget produced by rapid heating of powdery iron, iron oxide in slag and carbon mixture. *ISIJ International*. 2004;48(10):1368-72. <http://dx.doi.org/10.2355/isijinternational.48.1368>
- 15 Kim SH, Lee SH, Sasaki Y. Enhancement of iron rate the co-existence of graphite and Wüstite. *ISIJ International*. 2007;50(1):71-80. <http://dx.doi.org/10.2355/isijinternational.50.71>
- 16 Sasaki Y, Asano R, Ishii K. The effect of the liquid Fe-C phase on the kinetics in the carburization of iron by CO at 1523K. *ISIJ International*. 2001;41(3):209-15. <http://dx.doi.org/10.2355/isijinternational.41.209>
- 17 Murakami T, Fukuyama H, Nagata K. Mechanisms of carburization and melting of iron by CO gas. *ISIJ International*. 2001;41(5):416-21. <http://dx.doi.org/10.2355/isijinternational.41.416>

- 18 Fruehan RJ. The rate of carburization of iron in CO-H<sub>2</sub> atmospheres: Part I - Effect of temperature and CO and H<sub>2</sub>-pressures. Metallurgical Transactions. 1973;4:2123-27. <http://dx.doi.org/10.1007/BF02643276>
- 19 Iguchi Y, Endo S. Carburized carbon content of reduced iron and direct carburization in carbon composite iron ore pellets heated at elevated temperature. ISIJ International. 2004;44(12):1991-98. <http://dx.doi.org/10.2355/isijinternational.44.1991>
- 20 Hughe H, Davey J, Summerhill BD. The determination of metallic iron oxides pre-reduced ores. Londres: British Steel Corporation; 1976.
- 21 American Society for Testing and Materials - ASTM. E1019-11: Standard Test Methods for Determination of Carbon, Sulfur, Nitrogen, and Oxygen in Steel, Iron, Nickel, and Cobalt Alloys by Various Combustion and Fusion Techniques. ASTM; 2011.
- 22 Murakami T, Fukuyama H, Nagata K. Mechanisms of carburization and melting of iron by CO gas. ISIJ International. 2001;41(5):416-21. <http://dx.doi.org/10.2355/isijinternational.41.416>

Recebido em: 10/09/2013

Aceito em: 18/12/2013